Walk-Assist Robot: A Novel Approach to Gain Selection of a Braking Controller Using Differential Flatness

Chun-Hsu Ko, Kuu-Young Young, Yi-Che Huang, and Sunil K. Agrawal

***Abstract*— With increasing populations of the elderly in our society, robot technology will play an important role in providing functional mobility to humans. From the perspective of human safety, it is desirable that controllers for walk-assist robots be dissipative, i.e., the energy is supplied from the human to the walker, while the controller modulates this energy. The simplest form of a dissipating controller is a brake, where resistive torques are applied to the wheels proportional to their speeds. The fundamental question that we ask in this brief is how to modulate these proportional gains over time for the two wheels so that the walker can perform point-to-point motions. The unique contribution of this brief is a novel way in which the theory of differential flatness is used to plan the trajectory of these braking gains. Since the user input forces are not known *a priori*, the trajectory of the braking gain is computed iteratively during the motion. Simulation and experimental results show that the walk-assist robot, along with the structure of this proposed control scheme, can guide the user to reach the goal.**

***Index Terms*— Differential flatness, guidance, passive control, trajectory planning, walk-assist robot.**

I. Introduction

As THE population of the elderly grows rapidly, walk-assist robots continue to be an important research topic [1]–[3]. The aim of these works is to provide assistance to the elderly during walking and enhance their quality of life. Many walk-assist robots have been proposed to assist human walking [1]–[12]. Systems that support useful functions such as guidance [5], [7], [12], obstacle avoidance [8], [9], and health monitoring [1], [7] have been developed. In general, these robot walking helpers can be classified into two types, active and passive. The active robot walking helpers [1]–[5] use servo motors to provide guidance to the user while actively adding energy to the system. The passive walking helpers [8]–[11] move only by user-applied forces, and controlled brakes are used to steer the walker while constantly extracting energy out of the system. Passive walkers use dissipative control laws. With this property of energy dissipation, they are inherently safe and avoid energy buildup within the system. For a passive robot walking helper to be effective, it is important to appropriately control the braking torque in accordance with user-applied force so that it can be steered to the goal.

To control the robot walking helper, Spenko *et al*. [7] used a variable damping model to increase walking stability. Hirata *et al*. [8] proposed an adaptive motion control algorithm for obstacle avoidance and gravity compensation. Chuy *et al*. [9] used the passive behavior to enhance the interaction between the user and the support system. For effectively guiding the user, Agrawal *et al*. [10] proposed a passive control algorithm for the user to attain the desired position and orientation while allowing for small errors. Peshkin *et al*. [13] developed the passive assist system referred to as cobot, which uses active actuators that can accurately control the guidance direction by actively steering the wheels in response to user-applied forces. Passive haptic systems [14]–[16] use velocity or force controllers for path-following and guidance, but without considering system dynamics. For passive guidance of the robot walking helper, it needs to deal with robot walker's dynamics and also user-applied forces. It is quite challenging to efficiently derive proper brake torques during guidance. Optimal control methods, e.g., model predictive control [17], have been proposed for controlling active mobile robots. When applied to passive guidance, they may require repetitive integration of differential equations and solving brake torques constraints, which results in low efficiency. The differential flatness approach [18] deals with both trajectory planning and robot control within a common framework. It first plans the trajectories of the robot's flat outputs with a set of parameters and mode functions. The system dynamic equations and brake gain constraints can then be transformed into a set of algebraic equations, which are much easier to solve. The braking torques can thus be efficiently selected. This appealing feature motivates us to adopt it for passive guidance.

We apply a braking control law on the wheels to differentially steer a walking helper. This control law is both passive and dissipative. An open question is how to choose the braking gains for guidance. The novelty of this brief is in the use of the method of differential flatness to select time-varying trajectories of braking gains so that the vehicle achieves a desired final position and orientation. In this approach, the nonlinear structure of the vehicle dynamic equation under the braking control law is explored while using the property of differential flatness. In this model, the braking coefficients are treated as the new control inputs of the system. Once this

Manuscript received June 26, 2011; revised August 30, 2012; accepted November 26, 2012. Manuscript received in final form December 4, 2012. Date of publication January 11, 2013; date of current version October 15, 2013. This work was supported by the National Science Council, Taiwan, under Grant NSC 98-2918-I-214-001 and Grant NSC 96-2628-E-009-164-MY3. The work of S. K. Agrawal was supported in part by WCU Program. Part of this paper was presented at the American Control Conference July 1, 2010. Recommended by Associate Editor M. Zefran.

C.-H. Ko is with the Department of Electrical Engineering, I-Shou University, Kaohsiung 84001, Taiwan (e-mail: chko@isu.edu.tw).

K.-Y. Young and Y.-C. Huang are with the Department of Electrical Engineering, National Chiao Tung University, Hsinchu 300, Taiwan (e-mail: kyoung@mail.nctu.edu.tw; ychuang.ece96g@nctu.edu.tw).

S. K. Agrawal is with the Department of Mechanical Engineering, Columbia University, New York, NY 10027 USA.

Color versions of one or more of the figures in this paper are available online at http://ieeexplore.ieee.org.

Digital Object Identifier 10.1109/TCST.2012.2232668

1063-6536 © 2013 IEEE

Fig. 1. User pushing the robot walking helper for guidance.

property of differential flatness is demonstrated for the system under the braking control law, the states and inputs are represented as functions of flat outputs and their derivatives, and the trajectories of flat outputs are then planned. To efficiently select the braking gains, a passive guidance controller based on user-applied force is proposed. Since the time-varying user-applied forces are not known *a priori*, the braking gains are computed iteratively. Finally, simulations and experiments on this passive robot walker are performed to demonstrate the effectiveness of the proposed approach.

The remainder of this brief is organized as follows. Section II describes the dynamic equations of the passive robot walking helper. In Section III, differential flatness is briefly addressed. Guidance with passive control is described in Section IV. Sections V and VI present the simulation and experimental results, respectively. Finally, concluding remarks are given in Section VII.

II. Robot Walking Helper and its Model

The robot walking helper [11], shown in Fig. 1, consists of a support frame, two wheels with servo brakes, encoders, two passive casters, a force sensor, and a PC-based controller. The support frame has a semi-enclosed design that allows the user to walk at the center of the helper and provides support and stability. In order to obtain a high brake torque, a gear system with a 2.5 magnification is used between the servo brake and the rear wheel. The encoders are used to measure the wheel speed, while the force sensor detects the user-applied force. The servos provide proper braking force for controlling the motion of the robot walking helper. For controller design, we describe its dynamics next.

Fig. 2 shows its configuration in Cartesian coordinates [10], [19] given by

$$q = [x, y, \theta]^T \tag{1}$$

where x, y are the coordinates of the center of the rear axle, and θ is the heading angle of the robot. With the assumption of no slip at the wheel contact points, the velocity of the wheel

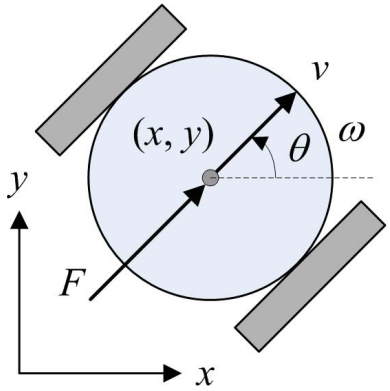

Fig. 2. Configuration of a passive robot walking helper.

centers are parallel to the heading direction. Hence, $\dot{q}$ can be expressed as

$$\dot{q} = S(q)V \tag{2}$$

where V is the vector of the heading speed υ and turning speed ω, i.e., $V = [\upsilon, \omega]^T$ and $S(q)$ is given by

$$S(q) = \begin{bmatrix} \cos\theta & 0 \\ \sin\theta & 0 \\ 0 & 1 \end{bmatrix}. \tag{3}$$

Assume that the robot walking helper is symmetric and the user applies a push force F on the robot along the forward direction. The equations of motion are thus given as

$$M\ddot{q} = E\tau + DF - C\lambda \tag{4}$$

where

$$M = \begin{bmatrix} m & 0 & 0 \\ 0 & m & 0 \\ 0 & 0 & I \end{bmatrix}, E = \begin{bmatrix} \cos\theta/r & \cos\theta/r \\ \sin\theta/r & \sin\theta/r \\ b/r & -b/r \end{bmatrix}, \tau = \begin{bmatrix} \tau_r \\ \tau_l \end{bmatrix},$$
$$D = \begin{bmatrix} \cos\theta \\ \sin\theta \\ 0 \end{bmatrix}, C = \begin{bmatrix} \sin\theta \\ -\cos\theta \\ 0 \end{bmatrix}. \tag{5}$$

Here, m is the mass of the walker, I is the moment of inertia about the center of the rear axle, r is the wheel radius, b is half-distance between the two wheels, τ_r and τ_l are the motor torques applied to the right and left wheels, respectively, and λ the constraint force. On differentiating (2), it leads to $\ddot{q} = \dot{S}V + S\dot{V}$. By substituting $\ddot{q}$ into (4) and premultiplying by S^T, we get

$$\dot{q} = SV$$
$$\dot{V} = (S^T MS)^{-1} S^T E\tau + (S^T MS)^{-1} S^T DF. \tag{6}$$

To make the robot passive and dissipative, we let the control law to be

$$\tau_r = -K_r\dot{\theta}_r, \qquad \tau_l = -K_l\dot{\theta}_l \tag{7}$$

where $\dot{\theta}_r$ and $\dot{\theta}_l$ are the angular speeds of the right and left wheels, respectively, and K_r and K_l are nonnegative parameters. With the no-slip condition, the angular speeds $\dot{\theta}_r$, $\dot{\theta}_l$ can be calculated as

$$\dot{\theta}_r = \frac{(\upsilon + b\omega)}{r}, \qquad \dot{\theta}_l = \frac{(\upsilon - b\omega)}{r}. \tag{8}$$

Substituting (7) and (8) into (6), we can obtain the dynamic equations of the passive robot as

$$\begin{aligned} \dot{q} &= SV \\ \dot{V} &= AK + BF \end{aligned} \tag{9}$$

where

$$A = \begin{bmatrix} -\frac{\upsilon+b\omega}{mr^2} & -\frac{\upsilon-b\omega}{mr^2} \\ -\frac{b(\upsilon+b\omega)}{Ir^2} & \frac{b(\upsilon-b\omega)}{Ir^2} \end{bmatrix}, \quad K = \begin{bmatrix} K_r \\ K_l \end{bmatrix}, \quad B = \begin{bmatrix} \frac{1}{m} \\ 0 \end{bmatrix}. \tag{10}$$

The nonnegative K can now be regarded as the new control inputs that need to be planned to steer the vehicle from its current state to the desired goal state. To design the feedback controller, we select the brake gain K by using the differential flatness approach, described in the next section.

III. Differential Flatness

In the differential flatness approach [18], [20], [21], a nonlinear dynamic equation is shown to be diffeomorphically equivalent to a linear system via static or dynamic feedback. For our system, there are two inputs, and hence we select two outputs such that the system becomes linear through input and state transformation via dynamic feedback. We select two suitable flat outputs and express all state variables and inputs in terms of the flat outputs and their derivatives. For the walking-assist robot, we find that the flat outputs $(y_1, y_2) = (x, y)$. The robot state variables can then be expressed as

$$\begin{aligned} (x, y) &= (y_1, y_2), \quad \theta = \arctan\left(\frac{\dot{y}_2}{\dot{y}_1}\right), \quad \upsilon = \sqrt{\dot{y}_1^2 + \dot{y}_2^2}, \\ \omega &= \frac{\dot{y}_1\ddot{y}_2 - \ddot{y}_1\dot{y}_2}{\dot{y}_1^2 + \dot{y}_2^2}, \quad \dot{\upsilon} = \frac{\dot{y}_1\ddot{y}_1 + \dot{y}_2\ddot{y}_2}{\sqrt{\dot{y}_1^2 + \dot{y}_2^2}}, \\ \dot{\omega} &= \frac{-\sin\theta\dddot{y}_1 + \cos\theta\dddot{y}_2 - 2\dot{\upsilon}\omega}{\upsilon}. \end{aligned} \tag{11}$$

Using (9)–(11), the control gain K can be expressed with the flat outputs and their derivatives as

$$K = G(\dot{y}_1, \ddot{y}_1, \dddot{y}_1, \dot{y}_2, \ddot{y}_2, \dddot{y}_2) \tag{12}$$

where

$$G = A^{-1}\left(\begin{bmatrix} \dot{\upsilon} \\ \dot{\omega} \end{bmatrix} - BF\right). \tag{13}$$

Note that K should be nonnegative for passive control. Because the user may push or pull the walking helper, the robot would experience the conditions of crossing the zero speed or zero force. When the wheel speed $\dot{\theta}_r$ or $\dot{\theta}_l$ becomes zero, A is singular and K cannot be obtained. Meanwhile, the detected user-applied force may be around zero or negative when the user pulls the walking helper. Under these conditions, the brake gain K is set to a positive constant to increase damping that stabilizes the system, which is realized via the servo brake. When the user pushes the walker to move forward with a positive wheel speed, passive guidance is activated utilizing trajectories of the flat outputs with the constraint of nonnegative control gain K, which is described in the next section.

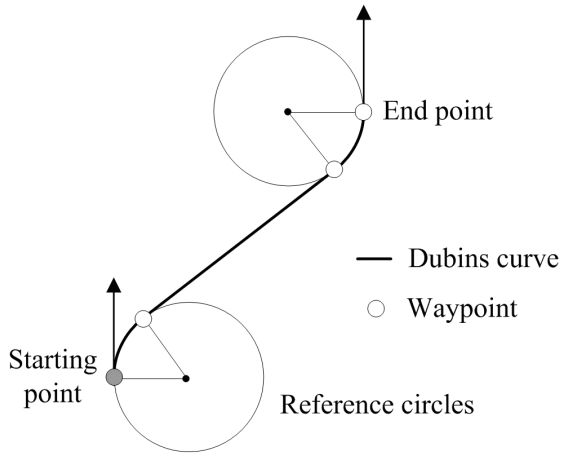

Fig. 3. Waypoints generation from Dubins curve.

IV. Guidance With Passive Control

Fig. 3 shows the proposed guidance control scheme for the passive robot with which a feasible trajectory and brake torques are calculated for the period t_f, given the current waypoint, measured states, and user-applied forces. Brake torques are then applied for controlling the robot when pushed by the user. This scheme uses a constant value of the current measured user-applied force. Therefore, the proposed approach only uses the brake torques to control the robot over a period of time Δt. At the next time step, it needs to read the states and user-applied forces, and generate a new trajectory. The procedure is repeated until the stop criterion is satisfied. Meanwhile, the robot guides the user walking through the consecutive waypoints. For this control scheme, the passive controller is designed using the differential flatness approach. With the approach, we first plan a smooth trajectory $[y_1(t), y_2(t)]$ that passes from the initial point to the end point. The robot state and brake gain K can thus be obtained. The time transform technique [22] is then applied to dynamically scale the trajectory such that the robot can reach the end point with positive brake gains.

To find a smooth trajectory, we first select a set of waypoints that can be connected into a smooth path using Dubins curve [23]. This consists of subpaths of arcs or straight lines to connect the waypoints. Fig. 4 shows an example of waypoints generation from the S-shaped Dubins curve. The robot can then guide the user to pass through these waypoints consecutively. In trajectory planning, the initial conditions $y_1(0), \dot{y}_1(0), \ddot{y}_1(0), y_2(0), \dot{y}_2(0), \ddot{y}_2(0)$ and the final conditions $y_1(t_f), \dot{y}_1(t_f), \ddot{y}_1(t_f), y_2(t_f), \dot{y}_2(t_f), \ddot{y}_2(t_f)$ of the trajectory can be calculated from the initial state $x(0), y(0), \theta(0), \upsilon(0), \omega(0)$ and the final state $x(t_f), y(t_f), \theta(t_f), \upsilon(t_f), \omega(t_f)$, with the parameters expressed as

$$\begin{aligned} y_1 &= x, \dot{y}_1 = \upsilon\cos\theta, \ddot{y}_1 = \dot{\upsilon}\cos\theta - \upsilon\sin\theta\omega \\ y_2 &= y, \dot{y}_2 = \upsilon\sin\theta, \ddot{y}_2 = \dot{\upsilon}\sin\theta + \upsilon\cos\theta\omega. \end{aligned} \tag{14}$$

The initial and final accelerations, $\dot{\upsilon}(0), \dot{\upsilon}(t_f)$, are set to be zeros, the final speed $\upsilon(t_f)$ is set to be the initial speed $\upsilon(0)$, and the final angular speed $\omega(t_f)$ is set to be zero. The trajectory can be fitted with the following polynomial

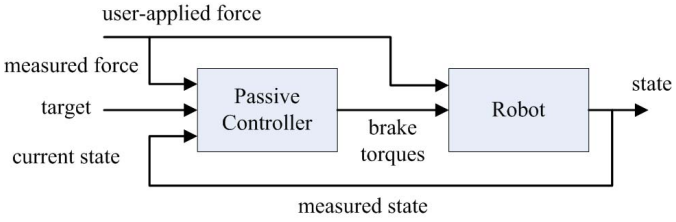

Fig. 4. Proposed guidance control scheme for passive robot.

function [24]:

$$y_j(t) = c_{j0} + c_{j1}t + c_{j2}t^2 + c_{j3}t^3 + c_{j4}t^3(t-t_f) + c_{j5}t^3(t-t_f)^2, \quad j = 1, 2. \tag{15}$$

Once the flat outputs are obtained using (15), the robot states and inputs can be represented as functions of t_f. The constant-speed trajectory $[y_1(t), y_2(t)]$ can then be obtained by solving the following nonlinear optimization problem:

$$\min_{t_f} J = \frac{1}{t_f}\int_0^{t_f} (v(t) - v(0))^2 dt \tag{16}$$

where J is the difference between the walking speed and the initial speed.

With the time transform method [22], the scaled trajectory $(y_1^s(t), y_2^s(t))$ is expressed as

$$y_1^s(t) = y_1(u(t)), \qquad y_2^s(t) = y_2(u(t)) \tag{17}$$

where $u(t)$ is the time transform function. The speed $v^s(t)$ of the scaled trajectory is calculated as $\dot{u}(t)v(t)$, where $v(t)$ is the speed of the constant-speed trajectory. The derivative $\dot{u}(t)$ of time transform function can be regarded as the speed scaling function, set as

$$\dot{u}(t) = (1-s)e^{-t/\alpha} + s \tag{18}$$

where s is the speed scaling parameter and α time constant. If $s > 1$, the speed $v^s(t)$ is increased; if $s < 1$, $v^s(t)$ is decreased. By integrating $\dot{u}(t)$ with $u(0) = 0$, the time transform function $u(t)$ can be obtained as

$$u(t) = \alpha(1-s)(1-e^{-t/\alpha}) + st. \tag{19}$$

The derivatives of the scaled trajectory are then calculated as

$$\begin{aligned} \dot{y}_j^s &= y_j^{'}\dot{u} \\ \ddot{y}_j^s &= y_j^{''}\dot{u}^2 + y_j^{'}\ddot{u} \\ \dddot{y}_j^s &= y_j^{'''}\dot{u}^3 + 3y_j^{''}\dot{u}\ddot{u} + y_j^{'}\dddot{u}, \qquad j = 1, 2. \end{aligned} \tag{20}$$

With (11), (12), and (20), the control gain K can be obtained. We then select the speed with the speed scaling parameter s to satisfy the nonnegative constraint of the control gain.

Since the passive guidance is performed with the positive wheel speed and positive force, the dimensionless passive index p with nonnegative control gain can be defined as

$$p = \min\left(\frac{K_r\dot{\theta}_r}{Fr}, \frac{K_l\dot{\theta}_l}{Fr}\right). \tag{21}$$

Algorithm 1 Passive Control Algorithm

Choose constants $\beta \in (0.5, 1)$, $\rho_d \in (0, 1)$, $\rho_i > 1$;
If $F < F_{\min}$ or $v < v_{\min}$, select positive constant gains to stabilize the system;
  let $K = K_c$;
Else, select positive gains for guidance;
  Fit the constant speed trajectory $(y_1(t), y_2(t))$ and calculate p, v, ω, K;
  If $p < p_{\min}$ or $v > \bar{v}$ or $\omega > \bar{\omega}$, the robot decreases speed;
    set $n = 0$;
    while ($p < p_{\min}$ and $n < n_{\max}$) or $v > \bar{v}$ or $\omega > \bar{\omega}$
      $n = n + 1$;
      calculate p, v, ω, K using the scaling trajectory $(y_1^s(t), y_2^s(t))$ with $s = \rho_d^n$;
    end
  Else, if $p > p_{\max}$ and $v < \beta\bar{v}$ and $\omega < \beta\bar{\omega}$, the robot increases speed;
    set $n = 0$;
    while $p > p_{\max}$ and $v < \beta\bar{v}$ and $\omega < \beta\bar{\omega}$ and $n < n_{\max}$,
      $n = n + 1$;
      calculate p, v, ω, K using the scaling trajectory $(y_1^s(t), y_2^s(t))$ with $s = \rho_i^n$;
    end
End

A larger positive p leads to a larger brake torque and a positive brake gain. With (9), the index p can be calculated as $p = \min(Fb - mb\dot{v} - I\dot{\omega},\ Fb - mb\dot{v} + \dot{\omega})/(2Fb)$. The angular acceleration $\dot{\omega}$ is obtained as $k\dot{v} + k'v^2$ with the trajectory curvature k and the derivative of curvature k' of the planned trajectory $(y_1(t), y_2(t))$. The passive index p can be further calculated as $p = \min(Fb - (mb - Ik)\dot{v} - Ik'v^2,\ Fb - (mb + Ik)\dot{v} + Ik'v^2)/(2Fb)$. Here, the curvature k is selected to satisfy $mb - I|k| > 0$. Hence, p can be nonnegative by properly selecting v and $\dot{v}$, which ensures nonnegative braking gain K.

When p is small or negative, the speed and acceleration should be reduced by selecting a small s value. On the other hand, when p is large and the speed is small, the speed can be increased by selecting a larger s value. Under the conditions when the user pulls the walker instead of pushing, or the speed is crossing zero, nonnegative brake gains for steering the vehicle to the desired goal may not be found. The positive constant gains are used to increase the damping within the system to maintain stability, while the system waits for an appropriate command from the user. Hence, the system under the proposed scheme maintains passivity and stability. Based on the discussion above, a passive control algorithm with the user-applied force is developed. Given the current robot state, user-applied force F, walking speed $\bar{v}$, angular speed $\bar{\omega}$, minimum force $F_{\min}$, minimum speed $v_{\min}$, the positive constant gains K_c, the minimum passive index value $p_{\min}$, the maximum passive index value $p_{\max}$, and the maximum iteration number $n_{\max}$, the brake gain K can be efficiently selected using in Algorithm 1.

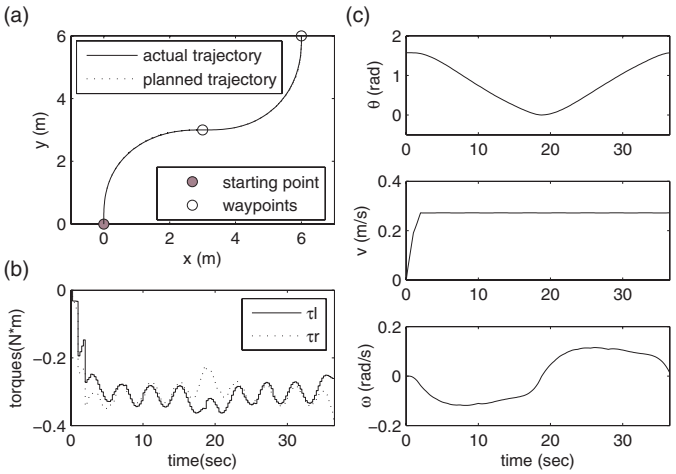

Fig. 5. S-shaped simulation results. (a) Actual and planned trajectories. (b) Brake torques. (c) Robot states.

V. Simulations

To evaluate the performance of the proposed scheme, it was first simulated for a passive robot walker for guidance. The parameter values of the robot were set to be $m = 50$ kg, $I = 11.56$ kg m^2, $r = 0.0616$ m, and $b = 0.34$ m. The user-applied force F was assumed to follow the function $f_p(1 + 0.1\sin(\pi \& t/2))$, with the sampling time Δt set as 0.25 s. The parameter values for the passive controller were set to be $\bar{v} = 0.3$ m/s, $\bar{\omega} = 0.2$ rad/s, $F_{\min} = 0.1$ N, $v_{\min} = 0.03$ m/s, $K_c = [0.08\ 0.08]$, $p_{\min} = 0.1$, $p_{\max} = 0.3$, $\beta = 0.9$, $\rho_d = 0.9$, and $\rho_I = 1.1$, and $n_{\max} = 100$.

The simulation of S-shaped guidance was performed with the mean user-applied force $f_p = 10$ N. The start and end points $(x_c,\ y_c,\ \theta)$ were set to be (0 m, 0 m, $\pi/2$ rad) and (6 m, 6 m, $\pi/2$ rad), respectively. Fig. 5(a) shows the actual and planned trajectories. It was observed that two waypoints were generated. The actual trajectory almost overlapped with the planned trajectory while approaching the target gradually. Fig. 5(b) shows the values of the torques τ_r, τ_l for S-shape guidance, which were all negative. Because the user-applied force was with oscillations, the torques τ_r, τ_l also show oscillations to compensate for the oscillating force to achieve stable walking. The trajectories of state θ, υ, ω of the guidance simulation are shown in Fig. 5(c). We observed that the walking speed was kept at about 0.27 m/s and the turning speed to within 0.2 rad/s. The simulation results show that the proposed scheme guided the user to the target stably and accurately. The robot would stop when the user stopped pushing. To evaluate the effect of the user-applied force, simulations with different values of mean force f_p were also conducted for S-shape simulations. The trajectories with f_p at 2, 5, and 20 N almost overlapped with f_p at 10 N [shown in Fig. 5(a)], indicating that the proposed scheme can still effectively guide the user under different user-applied forces.

VI. Experiments

For further evaluation, we performed the experiments for S-shaped guidance, with the experimental scenario shown in Fig. 1. Three users were invited and they were blind-folded to avoid visual feedback. Fig. 6 shows the robot trajectories during guidance, in which the robot guided the users to approach the waypoints. Table I shows the experimental results when the robot reached the position with $y = 6$. The x position errors of users A, B, and C are 0.64, 0.86, and 0.95 m, respectively, which might result from wheel slipping. The orientations θ of the three users are all close to the end-point orientation ($\pi/2$ rad). The speeds of the three users are 0.31, 0.26, and 0.33 m/s, respectively. Their mean values of user-applied force are about the same. Meanwhile, we also found that the force responses for these three users were similar. Fig. 7(a)–(c) shows the user-applied force, the brake torques, and the robot states in the S-shape experiment by user A, respectively. The robot applied torques τ_r, τ_l were all negative as expected. The trajectory of θ was smooth, the human walking speed was maintained within 0.42 m/s, and the turning speed was within 0.2 rad/s. These experimental results demonstrate that the proposed scheme can help the user to walk stably and guide the user to be close to the target.

The influence of user' mass variation on the performance was also evaluated. Table I lists users' masses for the

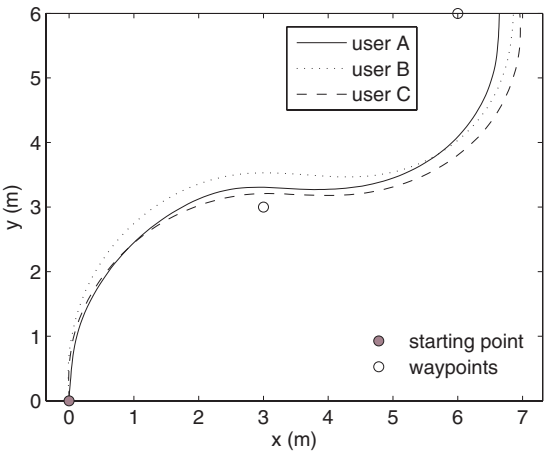

Fig. 6. Robot trajectories in S-shape experiments.

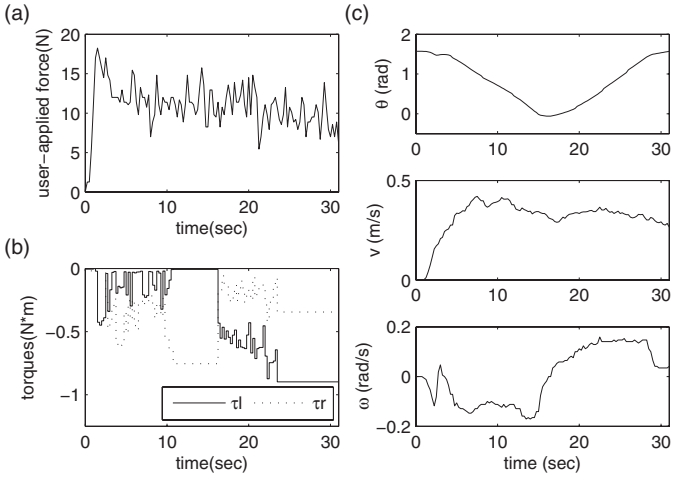

Fig. 7. S-shaped experimental results of user A. (a) User-applied force. (b) Brake torques. (c) Robot states.

TABLE I
USER MASS, POSITION (x, y, θ), MEAN OF SPEED, AND MEAN OF USER-APPLIED FORCE

	Mass (kg)	x(m)	y(m)	θ(rad)	Mean of Walking Speed (m/s)	Mean of User-Applied Force (N)
User A	64	6.64	6	1.56	0.31	10.84
User B	78	6.86	6	1.54	0.26	11.75
User C	70	6.95	6	1.65	0.33	11.66

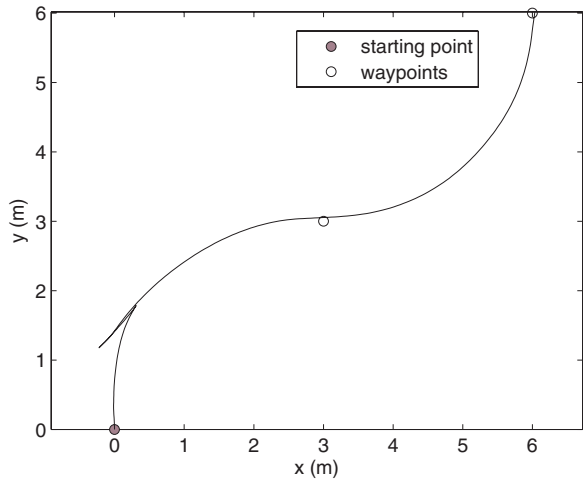

Fig. 8. Robot trajectory for S-shaped guidance with push-pull-push action.

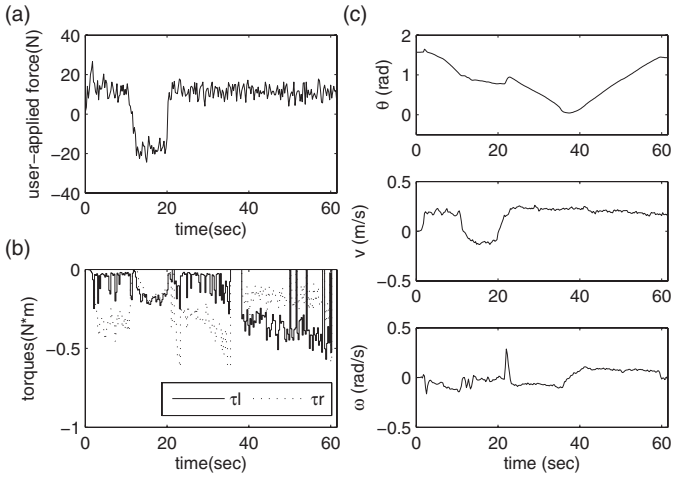

Fig. 9. Experimental results for S-shaped guidance with push-pull-push action. (a) User-applied force. (b) Brake torques. (c) Robot states.

experiments, i.e., 64, 78, and 70 kg, respectively. From the experimental results, the effect of mass variation on the performance was not evident. We consider that this walking helper is quite robust to users of ordinary weights to well-built ones. To further evaluate system stability, the experiments were performed for the case where the external force was not strictly positive. During the experiment for S-shape guidance, the user pushed the robot first, followed by a pull action, and then pushed it again. Fig. 8 shows the robot trajectory during guidance, in which the robot guided the user to approach the waypoints successfully. Fig. 9(a)–(c) shows the corresponding user-applied force, brake torques, and robot states, respectively. The brake torques τ_r, τ_l were all negative as expected even under the conditions of crossing the zero force or zero speed. From the results, the proposed algorithm maintains the system stability, when it waited for the push action from the user for guidance.

VII. CONCLUSION

In this brief, we presented a novel method for trajectory planning of the time-varying gains of a braking control law for a passive robot walking helper. The dynamic model of the vehicle with braking control law was first established. The trajectories of the gains were then developed by using approaches based on the theory of differential flatness. Accordingly, feasible trajectories were found by using the proposed passive guidance method. The trajectory of the braking gain is computed repetitively for the passive robot walking helper since user-applied forces are not known *a priori*. The simulation and experimental results showed that the passive robot walking helper with proposed guidance control scheme can guide the user to reach the goal, thereby demonstrating the effectiveness of the proposed scheme.

REFERENCES

[1] H. Yu, M. Spenko, and S. Dubowsky, "An adaptive shared control system for an intelligent mobility aid for the elderly," *Auto. Robots*, vol. 15, no. 1, pp. 53–66, Jul. 2003.
[2] O. Chuy, Y. Hirata, and K. Kosuge, "A new control approach for a robotic walking support system in adapting user characteristics," *IEEE Trans. Syst., Man Cybern. C, Appl. Rev.*, vol. 36, no. 6, pp. 725–733, Nov. 2006.
[3] A. J. Rentschler, R. A. Cooper, B. Blaschm, and M. L. Boninger, "Intelligent walkers for the elderly: Performance and safety testing of VA-PAMAID robotic walker," *J. Rehabil. Res. Develop.*, vol. 40, no. 5, pp. 423–432, 2003.
[4] G. Wasson, P. Sheth, M. Alwan, K. Granata, A. Ledoux, and C. Huang, "User intent in a shared control framework for pedestrian mobility aids," in *Proc. IEEE/RSJ Int. Conf. Intell. Robots Syst.*, Oct. 2003, pp. 2962–2967.
[5] J. Manuel, H. Wandosell, and B. Graf, "Non-holonomic navigation system of a walking-aid robot," in *Proc. IEEE Workshop Robot Human Interact. Commun.*, Sep. 2002, pp. 518–523.
[6] A. M. Sabatini, V. Genovese, and E. Pacchierotti, "A mobility aid for the support to walking and object transportation of people with motor impairments," in *Proc. IEEE/RSJ Int. Conf. Intell. Robots Syst.*, Oct. 2002, pp. 1349–1354.
[7] M. Spenko, H. Yu, and S. Dubowsky, "Robotic personal aids for mobility and monitoring for the elderly," *IEEE Trans. Neural Syst. Rehabil. Eng.*, vol. 14, no. 3, pp. 344–351, Sep. 2006.
[8] Y. Hirata, A. Hara, and. K. Kosuge, "Motion control of passive intelligent walker using servo brakes," *IEEE Trans. Robot.*, vol. 23, no. 5, pp. 981–990, Oct. 2007.
[9] O. Chuy, Y. Hirata, Z. Wang, and K. Kosuge, "A control approach based on passive behavior to enhance user interaction," *IEEE Trans. Robot.*, vol. 23, no. 5, pp. 899–908, Oct. 2007.
[10] J. C. Ryu, K. Pathak, and S. K. Agrawal, "Control of a passive mobility assist robot," *J. Medicial Devices*, vol. 2, no. 1, p. 011002, 2008.
[11] S. H. Yu, C. H. Ko, and K. Y. Young, "On the design of a robot walking helper with human intension and environmental sensing," in *Proc. CACS Int. Auto. Cont. Conf.*, 2008, pp. 1–28.
[12] C. H. Ko, K. Y. Young, Y. C. Huang, and S. K. Agrawal, "Active and passive control of walk-assist robot for outdoor guidance," *IEEE/ASME Trans. Mech.*, vol. PP, no. 99, pp. 1–10, Jul. 2012.
[13] M. A. Peshkin, J. E. Colgate, W. Wannasuphoprasit, C. A. Moore, R. B. Gillespie, and P. Akella, "Cobot architecture," *IEEE Tran. Robot. Autom.*, vol. 17, no. 4, pp. 377–390, Aug. 2001.

[14] D. K. Swanson and W. J. Book, "Path-following control for dissipative passive haptic displays," in *Proc. 11th Symp. Haptic Inter. Virtual Environ. Teleoperator Syst.*, Mar. 2003, pp. 101–108.

[15] B. Dellon and Y. Matsuoka, "Path guidance control for a safer large scale dissipative haptic display," in *Proc. IEEE Int. Conf. Robot. Autom.*, May 2008, pp. 2073–2078.

[16] C. H. Cho, J. B. Song, and M. S. Kim, "Energy-based control of a haptic device using brakes," *IEEE Trans. Syst., Man, Cybern. B, Cybern.*, vol. 37, no. 2, pp. 341–349, Apr. 2007.

[17] D. Gu and H. Hu, "Receding horizon tracking control of wheeled mobile robots," *IEEE Trans. Cont. Syst. Technol.*, vol. 14, no. 4, pp. 743–749, Jul. 2006.

[18] H. Sira-Ramirez and S. K. Agrawal, *Differential Flat Systems*. 1st ed. New York: Marcel Dekker, 2004.

[19] K. Pathak and S. K. Agrawal, "An integrated path-planning and control approach for nonholonomic unicycles using switch local potentials," *IEEE Tran. Robot.*, vol. 21, no. 6, pp. 1201–1208, Dec. 2005.

[20] J. C. Ryu, S. K. Agrawal, and J. Franch, "Motion planning and control of a tractor with a steerable trailer using differential flatness," *J. Comput. Nonlinear Dynamics*, vol. 3, pp. 031003-1–031003-8, Jul. 2008.

[21] C. P. Tang, P. T. Miller, V. N. Krovi, J. C. Ryu, and S. K. Agrawal, "Differential-flatness-based planning and control of a wheeled mobile manipulator-theory and experiment," *IEEE/ASME Trans. Mechatron.*, vol. 16, no. 4, pp. 768–773, Aug. 2011.

[22] M. Fliess, J. Lévine, P. Martin, and P. Rouchon, "Design of trajectory stabilizing feedback for driftless flat systems," in *Proc. 3rd Eur. Control Conf.*, 1995, pp. 1882–1887.

[23] S. M. LaValle, *Planning Algorithm*. Cambridge, U.K.: Cambridge Univ. Press, 2006.

[24] S. K. Agrawal and T. Veeraklaew, "A higher-order method for dynamic optimization of a class of linear systems," *J. Dynamic Syst., Meas., Control*, vol. 118, no. 4, pp. 786–791, Dec. 1996.